Agricultural Sciences, 2024, 15, 1018-1034
https://www.scirp.org/journal/as
ISSN Online: 2156-8561
ISSN Print: 2156-8553

Estimating the Yield Loss of Winter Wheat from Drought in the United States Southern Plains Region as Influenced by El Niño-Southern Oscillation (ENSO)

Prem Woli*, Gerald R. Smith, Charles R. Long, Francis M. Rouquette, Jr.

Texas A&M AgriLife Research Center, Overton, USA
Email: *prem.oli@ag.tamu.edu

How to cite this paper: Woli, P., Smith, G.R., Long, C.R. and Rouquette, Jr., F.M. (2024) Estimating the Yield Loss of Winter Wheat from Drought in the United States Southern Plains Region as Influenced by El Niño-Southern Oscillation (ENSO). *Agricultural Sciences*, **15**, 1018-1034.
https://doi.org/10.4236/as.2024.159055

Received: August 2, 2024
Accepted: September 16, 2024
Published: September 19, 2024

Abstract

Wheat (*Triticum aestivum* L.) production is a major economic activity in most regional and rural areas in the Southern Plains, a semi-arid region of the United States. This region is vulnerable to drought and is projected to experience a drier climate in the future. Since the interannual variability in climate in this region is linked to an ocean-atmospheric phenomenon, called El Niño-Southern Oscillation (ENSO), droughts in this region may be associated with ENSO. Droughts that occur during the critical growth phases of wheat can be extremely costly. However, the losses due to an impending drought can be minimized through mitigation measures if it is predicted in advance. Predicting the yield loss from an imminent drought is crucial for stakeholders. One of the reliable ways for such prediction is using a plant physiology-based agricultural drought index, such as Agricultural Reference Index for Drought (ARID). This study developed ENSO phase-specific, ARID-based models for predicting the drought-induced yield loss for winter wheat in this region by accounting for its phenological phase-specific sensitivity to drought. The reasonable values of the drought sensitivity coefficients of the yield model for each ENSO phase (El Niño, La Niña, or Neutral) indicated that the yield models reflected reasonably well the phenomena of water stress decreasing the winter wheat yields in this region during different ENSO phases. The values of various goodness-of-fit measures used, including the Nash-Sutcliffe Index (0.54 to 0.67), the Willmott Index (0.82 to 0.89), and the percentage error (20 to 26), indicated that the yield models performed fairly well at predicting the ENSO phase-specific loss of wheat yields from drought. This yield model may be useful for predicting yield loss from drought and scheduling irrigation allocation based on the phenological phase-specific sensitivity to drought as

impacted by ENSO.

Keywords

ARID, Drought, Drought Index, ENSO, El Niño, Growth-Stage, Model, Phenological-Phase, Prediction, Semi-Arid, Wheat, Yield Loss

1. Introduction

The semi-arid region encompassing eastern New Mexico and northwestern Texas, commonly known as Llano Estacado [1], is situated in the Southern Plains ecoregion of the United States [1]. This region is vulnerable to both frequent and flash droughts, which may occur during any time of the year. When the shortage of precipitation is combined with high temperatures, drought can develop quickly. This region is expected to experience a drier climate in the future because of global warming [2]. The elevated temperatures in this region will lead to a greater potential for more intense droughts [3]-[5] and a longer dry period between two rain events [6]. Due to global warming, food and forage production in this region is expected to decline not only through the increased frequency and duration of drought but also through the increased levels of soil moisture evaporation, crop stress, and water demand caused by elevated temperatures [7]. As temperatures rise beyond their preferred heat tolerance levels, many commodity crops are expected to experience yield declines even with irrigation. Milder winters and precipitation shifts caused by global warming will possibly escalate the incidence of pests and diseases for crops and livestock, whereas extreme heat is likely to reduce livestock productivity [7]. This region, especially the heavily irrigated areas which have already been plagued by unsustainable water use, will experience further stresses on water supply due to continued urbanization [8].

In most rural and regional areas of this region, wheat (*Triticum aestivum* L.) production is one of the predominant economic activities [9]. The majority of wheat growers across the region depend on rain for their crops. Droughts, especially the ones that occur during the critical phenological phases of wheat, can be very costly.

The losses due to an impending drought can be minimized through appropriate mitigation measures if it is predicted in advance [10] [11]. Predicting yield loss from an imminent drought is an important need of stakeholders. The ability to predict yield loss can help them with decisions regarding applying appropriate mitigation measures. The drought-induced yield losses may be predicted using various models that are based on techniques such as linear regressions, artificial neural network, fuzzy-logic inference system, random forest, time series analysis, remote sensing-based vegetation indices, and drought indices [10]-[12]. Relative to other methods, the drought indices are simpler, usually represented by a number; yet they provide a comprehensible big picture on drought conditions by

integrating all relevant information into that number.

Several drought indices are available for monitoring or predicting an agricultural drought, a temporary condition where the amount of plant available water in the soil due to precipitation falls short of the consumptive demand of crops [10] [11] [13]. However, only a plant physiology-based drought index can predict the yield loss due to drought more accurately, as yield formation is a plant physiological process [13]. One of such few indices is the Agricultural Reference Index for Drought (ARID), which can characterize an agricultural drought better than can many similar indices [13] [14]. The ARID is computed on a daily basis as the ratio of plant water deficit to plant water need, and its values range from 0 (no water stress) to 1 (full water stress).

Considering that a crop yield model that takes into account a series of phenological phases during the crop growing season could better reflect the effect of water stress on yield, [15] developed Equation (1) for estimating the water-stressed yield relative to the non-water-stressed yield, hereafter referred to as the relative yield ($\tilde{Y}$), and, eventually, the fraction of yield loss due to drought (1 – $\tilde{Y}$) for a determinate, flowering crop using the phenological phase-specific values of ARID.

$$\tilde{Y} = \prod_{p=1}^{P} \left(1 - \mathrm{ARID}\right)_{p}^{\lambda_p}, \tag{1}$$

where $\tilde{Y}$ is the relative yield of a crop, the symbol Π indicates a product, "p" is a phenological phase, "P" is the total number of phases considered during the crop season, and λ_p is the relative sensitivity of the crop to drought stress during the p-th phenological phase.

One of the crucial factors defining an agroecosystem's productivity is weather, and that defining a region's interannual variability in crop production is climate. In the southeastern United States, the yearly fluctuation of climate has been linked to an ocean-atmosphere phenomenon occurring across the equatorial Pacific Ocean, known as the El Niño-Southern Oscillation (ENSO) [16] [17]. The ENSO phenomenon has significantly affected crop production in this region [18]. Thanks to the strong connection between weather patterns in this region and ENSO, an ENSO phase may be successfully forecast up to a year in advance [19]. The ENSO-based forecast of weather conditions may reduce climate uncertainty for improved crop production.

In the Llano Estacado region, [20] as well as [21] found a strong association between winter wheat yields and ENSO. By estimating the λ_p values (Equation (1)) for various phenological phases of winter wheat, [22] developed the relative yield model for this crop for the Llano Estacado region. However, as the model is generic in terms of reflecting the climate variability effects, it does not represent the ENSO phase (El Niño, La Niña, and Neutral)-specific relationships between drought and wheat yields. In the southeastern United States, the El Niño years are generally wetter than usual during fall through spring [23]-[25] and the La Niña years tend to be wetter during summer and drier during winter and spring [26].

Because the weather patterns during different times of the year or different phenological phases of wheat are different under different phases of ENSO, the ENSO phase-specific yield model might represent the drought-yield relationship better than the generic yield model.

This study developed ENSO phase-specific, ARID-based yield models to predict the drought-induced yield loss for winter wheat in the Llano Estacado region of the southern United States. Specifically, the study estimated the phenological phase-specific drought sensitivity coefficients for various phenological phases of winter wheat to be used in the ENSO phase-specific relative yield models (Equation (2)).

$$\tilde{Y}_i = \prod_{p=1}^{P} \left(1 - \mathrm{ARID}\right)_{i,p}^{\lambda_{i,p}}, \tag{2}$$

where $\tilde{Y}_i$ is the ENSO phase-specific relative yield of winter wheat; the subscripts i and p stand for the i-th ENSO phase and the p-th phenological phase, respectively; P is the total number of phenological phases considered during the wheat season; and $\lambda_{i,p}$ is the relative sensitivity of winter wheat to drought stress during the p-th phenological phase under the i-th ENSO phase.

2. Materials and Methods

This study is a sequel to a previous study [22] that developed a generic yield model for winter wheat for the Ilano Estacado region with no regard to the ENSO phase. This sequel study developed ENSO phase-specific yield models for the same region by using the same data and procedures used by [22] and then splitting the data by the ENSO phase. The materials and methods used in [22] are summarized in Section 2.1 below.

2.1. Computing Phenological Phasic Values of ARID

Considering the availability of both irrigated and unirrigated yield data of winter wheat, Bushland, TX and Clovis, NM were selected as the representative locations for the Llano Estacado region. Then, their winter wheat yield data generated through variety trials conducted in multiple years (**Table 1**) under both irrigated and dryland conditions were obtained. The yields of all the winter wheat varieties used in the trials at each location in each year under each farming regimen (dryland or irrigated) were averaged to calculate the dryland and irrigated yields of a general winter wheat variety for these locations and years. Then, the relative yield of winter wheat for the corresponding location and year was calculated as the ratio of the dryland yield to the irrigated yield. The intent of using the relative yield was to reflect the effect of water only, while eliminating the effects of the other inputs involved, as both dryland and irrigated crops involved in each experiment had received the same amounts of other inputs, except the water.

Considering the availability of phase duration data and the approach used by [27], five phenological phases were included in this study: 1) planting-emergence (PE); 2) emergence-tillering (ET); 3) tillering-booting (TB); 4) booting-anthesis

(BA); and 5) anthesis-maturity (AM). Due to the lack of corresponding planting date data, representative planting dates from the literature were used (Bushland: 21 October, Clovis: 15 October). The duration of each phenological phase needed for splitting a growing season into several phases was estimated using the total thermal time (TTT; ˚C d) needed for each phase under dryland conditions (Table 2) [28]-[32]. Once the planting date for each location and the duration for each phase in each year at each location were estimated, each wheat growing season at each location was split into the five phenological phases described above.

Table 1. Years for which both dryland and irrigated winter wheat yield data were available at two locations in the Llano Estacado region of the southern USA under each ENSO phase.

ENSO Phase	Location	Seasons	Years
El Niño	Bushland, TX	14	1958, 1964, 1966, 1970, 1973, 1977, 1987, 1988, 1992, 1998, 2007, 2010, 2016, 2019
	Clovis, NM	14	1964, 1970, 1973, 1977, 1983, 1987, 1988, 1992, 1998, 2007, 2010, 2015, 2016, 2019
La Niña	Bushland, TX	9	1968, 1972, 1975, 1999, 2000, 2008, 2011, 2018, 2021
	Clovis, NM	11	1968, 1971, 1972, 1975, 1976, 1989, 1999, 2000, 2008, 2011, 2018
Neutral	Bushland, TX	26	1947, 1953, 1954, 1959, 1960, 1962, 1979, 1980-1982, 1985, 1986, 1990, 1991, 1994-1997, 2001, 2002, 2004, 2006, 2009, 2012, 2017, 2020
	Clovis, NM	22	1962, 1963, 1969, 1978-1982, 1984-1986, 1990, 1991, 1993-1997, 2001, 2005, 2006, 2017

Table 2. The total thermal time (TTT) needed to complete each phenological phase of winter wheat under dryland farming conditions in the Llano Estacado region of the southern USA.

Phenological phase (p)	TTT (˚C d)
Planting-emergence ($p = 1$)	150
Emergence-tillering ($p = 2$)	200
Tillering-booting ($p = 3$)	1152
Booting-anthesis ($p = 4$)	261
Anthesis-maturity ($p = 5$)	640

For each location, the daily values of ARID for each wheat growing season that had yield data were computed from the daily weather data, using the ARID equations described by [13] and the computational procedure (MATLAB program) provided by [10]. Once the daily values of ARID were computed for each year at each location, they were averaged by the phenological phase. The phasic values of ARID were then converted into the corresponding phasic values of "1 − ARID" as the yield model (Equation (1)) needs the latter.

2.2. Classifying ENSO Years

For developing the ENSO phase-specific yield models, the years for which yield

data were available (Table 1) were assigned to a specific ENSO phase as categorized by the Japan Meteorological Agency (JMA) index [33]-[36]. The JMA index is a 5-month moving average of the sea surface temperature anomalies over the Equatorial Pacific (4˚S - 4˚N, 150˚W - 90˚W). An ENSO year, which starts from October through the following September, is categorized as El Niño, La Niña, or Neutral if the index values are ≥0.5˚C, ≤−0.5˚C, or between −0.5˚C and 0.5˚C, respectively, for 6 consecutive months, including October, November, and December [34] [36]. For ENSO characterization, the JMA index was used as it selects the ENSO events better than other similar indices [36]. According to this index, the total number of years for which the yield data were available in the Llano Estacado region (Bushland plus Clovis) under the El Niño, La Niña, and Neutral phases of ENSO were 28, 20, and 48, respectively (Table 1).

2.3. Developing the ENSO Phase-Specific Yield Models

Once the relative yield values of wheat and the phenological phasic values of (1 − ARID) were calculated for each year in each location under each ENSO phase, a matrix of dataset comprising 28 rows (years) and six columns was prepared for El Niño, that comprising 20 rows and six columns for La Niña, and that comprising 48 rows and six columns for the Neutral phase. The first column in the matrix contained the relative yields (dependent variable), and the remaining columns contained the corresponding phenological phasic values of (1 − ARID) for the five phases (independent variables).

For developing the ENSO phase-specific yield models, estimating the drought-sensitivity coefficient for winter wheat during the phenological phase p, denoted as λ_p, for each ENSO phase would be necessary. This would require regressing the linearized form (Equation (3)) of the ENSO phase-specific yield model (Equation (2)). Accordingly, all the values in the matrix prepared for each ENSO phase as explained above were converted to the natural logarithmic (ln) values. These transformed matrices, in turn, were used in the R-project software (https://www.r-project.org/) to estimate the λ_p values through multiple linear regressions. The linearized yield model is as follows.

$$\ln\left(\tilde{Y}_{i,j,k}\right) = \sum_{p=1}^{P}\left\{\lambda_{i,p} \times \ln\left(1-\mathrm{ARID}_{i,j,k,p}\right)\right\}, \tag{3}$$

where $\tilde{Y}_{i,j,k}$ is the relative yield; P is the total number of phenological phases of winter wheat considered (5); and the subscripts i, j, k, and p stand for the i-th ENSO phase, the j-th location, the k-th year, and the p-th phenological phase, respectively.

2.4. Evaluating the ENSO Phase-Specific Yield Models

Given the limited number of years available, especially for the El Niño and La Niña phases, the leave-one-out technique of cross-validation was used to evaluate the yield model. Following this technique, the available dataset (the transformed matrix) for each ENSO phase was divided into two parts: one for parameterization

and the other for evaluation. That is, of the total 28 input-output combinations for El Nino, for instance, the first 27 combinations (rows) were used as the parameterization set for estimating the λ_P values through the regression of Equation (3) and the last one combination (row) as the evaluation set for yield estimation through the use of the just estimated $\lambda_{i,P}$ values in the yield model (Equation (2)). Leaving one combination out and adding one combination in, both parameterization and the evaluation sets were moved forward 27 times. Each movement created a new parameterization set and a new evaluation set, which, in turn, produced a set of new λ_P values through regressions (using Equation (3)) and, finally, a yield estimate (using Equation (2)). This process, consequently, provided 28 relative yield estimates for El Niño, 20 for La Niña, and 48 for the Neutral phase. Finally, using the mean absolute error, the root mean square error (RMSE), the Nash-Sutcliffe Index [37], and the Willmott Index [38] as the measures of fit, the estimated relative yields using Equation (2) for the years for which the observed yields were available under each ENSO phase were compared with the corresponding observed relative yields to evaluate the performance of an ENSO phase-specific winter wheat yield model.

3. Results and Discussion

3.1. ENSO Phase-Specific Yield Models

Table 3 shows the phenological phase-specific drought sensitivity coefficients estimated for the ENSO phase-specific winter wheat yield model (Equation (2)) for the Llano Estacado region of the United States. Using these coefficients in Equation (2) resulted in the following ENSO phase-specific relative yield models for winter wheat.

$$\tilde{Y}_E = 1.21\times(1-\mathrm{ARID})_{E,\mathrm{PE}}^{0.03}\times(1-\mathrm{ARID})_{E,\mathrm{ET}}^{0.082}\times(1-\mathrm{ARID})_{E,\mathrm{TB}}^{0.443}\times(1-\mathrm{ARID})_{E,\mathrm{BA}}^{0.043}\times(1-\mathrm{ARID})_{E,\mathrm{AM}}^{0.039} \quad (4)$$

$$\tilde{Y}_L = 0.67\times(1-\mathrm{ARID})_{L,\mathrm{PE}}^{0.037}\times(1-\mathrm{ARID})_{L,\mathrm{ET}}^{0.066}\times(1-\mathrm{ARID})_{L,\mathrm{TB}}^{0.165}\times(1-\mathrm{ARID})_{L,\mathrm{BA}}^{0.075}\times(1-\mathrm{ARID})_{L,\mathrm{AM}}^{0.023} \quad (5)$$

$$\tilde{Y}_N = 0.99\times(1-\mathrm{ARID})_{N,\mathrm{PE}}^{0.03}\times(1-\mathrm{ARID})_{N,\mathrm{ET}}^{0.167}\times(1-\mathrm{ARID})_{N,\mathrm{TB}}^{0.263}\times(1-\mathrm{ARID})_{N,\mathrm{BA}}^{0.154}\times(1-\mathrm{ARID})_{N,\mathrm{AM}}^{0.019} \quad (6)$$

where $\tilde{Y}_E$, $\tilde{Y}_L$, and $\tilde{Y}_N$ are the relative yields of winter wheat for the El Niño (*E*), La Niña (*L*), and Neutral (*N*) phases of ENSO, respectively; and the five phenological phases are represented by subscripts PE, ET, TB, BA, and AM.

All the sensitivity coefficients under each ENSO phase had positive values, indicating that the water stress during any phenological phase of winter wheat would have negative impacts on yields under any ENSO phase. This result was in agreement with the findings of several previous studies. In a similar study conducted in the Llano Estacado region, but without considering the ENSO effect, [22] also found that water stress during any phase could be detrimental. In an experiment carried out in Arizona, USA, [39] observed that wheat grain yields were reduced by the water stress that occurred at any growth stage. In a review study, [27] demonstrated that wheat yields could be impacted by water stress during any phenological phase, depending on the weather conditions. Reference [40]

also exhibited through a review paper that winter wheat yield is vulnerable to drought at any growth stage. Reference [41] promulgated that water stress occurring at any particular stage would result only in high yield losses, not crop failure, whereas that occurring during the entire growing season would result in crop failure.

Table 3. The drought sensitivity coefficient (λ_P) values for various phenological phases of winter wheat in the Llano Estacado region of the United States under three ENSO phases.

Phenological phase	λ_P	ENSO phase		
		El Niño	La Niña	Neutral
	Intercept	1.210	0.670	0.990
Planting-emergence (PE)	λ_1	0.030	0.037	0.030
Emergence-tillering (ET)	λ_2	0.082	0.066	0.167
Tillering-booting (TB)	λ_3	0.443	0.165	0.263
Booting-anthesis (BA)	λ_4	0.043	0.075	0.154
Anthesis-maturity (AM)	λ_5	0.039	0.023	0.019

Under each ENSO phase, the TB phenological phase had the largest value of the drought sensitivity coefficient of all the phenological phases of winter wheat considered (**Table 3**), implying that this phenological phase was the most sensitive to drought. This implication was consistent with those of several other studies [22] [27] [39] [41] [42]. The likely reasons for the greatest sensitivity of winter wheat yields to drought during the TB phase were as follows. The crop water demand during this phenological phase is high [43]. The water stress during this phase reduces the number of stems and heads by increasing the senescence of tillers and stems and reduces yields by reducing the number of grains through fewer spikelets per head, fewer grains per spikelet, or both [27] [39] [44] [45].

The ET phase was the second most sensitive phase to drought under El Niño and Neutral and the third most sensitive phase under La Niña. The following phenomena were possible causes for high drought sensitivity during this phase. Plant water stress during the ET phase drastically limits leaf growth and tiller development [44] [46]-[50]. Under severe water stress, tillering may decrease by about 50% [47] [49], and leaf area index (LAI) development is severely hampered [27]. Water stress just before floral initiation decreases the number of spikelet primordia [51].

In drought sensitivity, the BA phase followed the ET phase under El Niño and Neutral and the TB phase under La Niña. The sensitivity of wheat yields to drought during the BA phase was likely due to the following phenomena. Plant water stress during this phase reduces the availability of carbon and nitrogen, both of which are critical for spike growth [27]. When water stress occurs during spike growth and emergence, the kernel number decreases sharply, leading to a decrease in wheat yields at a maximum rate [52]. Water stress at heading increases the

number of sterile spikelets and florets and that around anthesis affects pollination and fertilization, thus reducing the seed setting rate and, eventually the grain yield [50]. Water stress during this phase reduces yields also through insufficient assimilates [53].

As the sensitivity coefficients under all ENSO phases showed, the PE phase was less sensitive to drought than ET, TB, and BA phases. References [22] and [41] also found similar results. The sensitivity of wheat yields during PE was likely because an early drought in the growing season may have affected wheat germination and crop establishment [54]. Severe water stress during PE and ET prevents crop development [27].

The smaller values of the drought sensitivity coefficients during the AM phase relative to other phenological phases under all ENSO phases indicated that winter wheat yields were the least sensitive to drought that occurred during this phenological phase in any ENSO year. The scientific documentation also shows that, of all the phenological phases of wheat, water stress during the AM phase had the smallest yield impacts [39] [42]. The detrimental effect of drought on wheat yields during this phase was likely because the water stress around anthesis decreased carbohydrate accumulation in the stem by accelerating development [55] [56] and during grain-filling shortened the grain-filling period by accelerating senescence [52] [57]. The terminal part of the grain-filling period in the Llano Estacado region is generally hot and dry, which tends to terminate grain-filling early. Under these conditions, more grains may be more important than a greater grain-filling rate during the AM phase for high yields [44]. The larger sensitivity coefficients for TB and BA phases relative to the AM phase well reflected this phenomenon (**Table 3**). The rational values of the sensitivity coefficients suggested that the yield models (Equations (4) to (6)) were able to express the ENSO phase-specific relationship between ARID and the relative yields of winter wheat in the Llano Estacado region accurately.

As **Table 3** shows, the order of phenological phases with diminishing sensitivity to drought under a given ENSO phase was as follows. El Nino: TB > ET > BA > AM > PE. La Niña: TB > BA > ET > PE > AM. Neutral: TB > ET > BA > PE > AM. However, the coefficient values, especially between ET and BA phases, were not significantly different under each ENSO phase. Also, the coefficient difference between PE and AM phases was not significant under each ENSO phase. These patterns suggested that in terms of drought sensitivity, the five phenological phases studied could be classified into three groups: 1) highly sensitive: TB; 2) moderately sensitive: ET and BA; and 3) slightly sensitive: PE and AM.

3.2. The Performance of the Yield Models

The values of the various metrics used to evaluate the performance of the ENSO phase-specific winter wheat yield models for the Llano Estacado region of the southern United States are presented in **Table 4**. The RMSE value ranged from 0.07 to 0.10 (dryland yield per unit of irrigated yield), whereas the mean absolute

error value ranged from 0.06 to 0.09. The percentage error of the yield model, computed as the ratio of RMSE to the mean observed relative yield, ranged from 20 to 26. The value of the Willmott index fell between 0.82 and 0.89, whereas that of the Nash-Sutcliffe index lay between 0.54 and 0.67. As the values of these metrics indicated, each ENSO phase-specific winter wheat yield model performed reasonably well at predicting the relative yields and, thus, the yield losses due to drought.

Table 4. The values of the various measures used to evaluate the performance of the ENSO phase-specific winter wheat yield models in the Llano Estacado region of the United States.

Measures	ENSO phase		
	El Niño	La Niña	Neutral
Mean observed relative yield	0.52	0.32	0.37
Mean predicted relative yield	0.52	0.32	0.37
Mean absolute error	0.09	0.06	0.08
Root mean square error	0.10	0.07	0.10
Willmott Index	0.82	0.89	0.87
Nash-Sutcliffe Index	0.54	0.67	0.62
Percentage error	20	23	26

The Willmott index values indicated that the relative yields of winter wheat estimated by the yield model agreed fairly closely with those calculated from the observed data. The Nash-Sutcliffe index values also indicated that the agreements between the model-estimated and observed values were acceptable for the winter wheat yield model, and thus the predictive power of the yield model was relatively good. As the positive values of this index indicated, the model predictions were more accurate than the means of the observed data. The mean values of both observed and relative yields were the same and ranged from 0.32 to 0.52 across the ENSO phase-specific models. The percentage error, if computed as the absolute difference between the predicted and the observed values relative to the observed value, would be almost zero, an indication of a small error. Under El Niño, the range of the predicted relative yields was 0.27 to 0.68, and that of the observed relative yields was 0.25 to 0.78. That is, the width of the range of the predicted yields (0.41) relative to that of the observed yields (0.53) was about 0.77, which indicated that the model error based on this statistic was about 23%. Similarly, the errors of this kind under La Niña and Neutral were 24% and 14%, respectively. These values were also an indication for a relatively low modeling error. All the above metrics indicated that each ENSO phase-specific yield model was able to reflect the phenomenon of water stress decreasing the yields of winter wheat in the Llano Estacado region fairly well (**Figure 1**).

The performance of each ENSO phase-specific yield model was significantly better than that of the generic yield model [22], which did not consider the ENSO effects (**Table 4** vs. **Table 5**). Compared with the generic model, the ENSO phase-

specific models increased the Willmott index by 0% to 9% and the Nash-Sutcliffe index by 14% to 28%, depending on the ENSO phase. Similarly, the ENSO-specific yield models reduced the mean absolute error by 5% to 11% and the percentage error and the root mean square error by 11% to 12%.

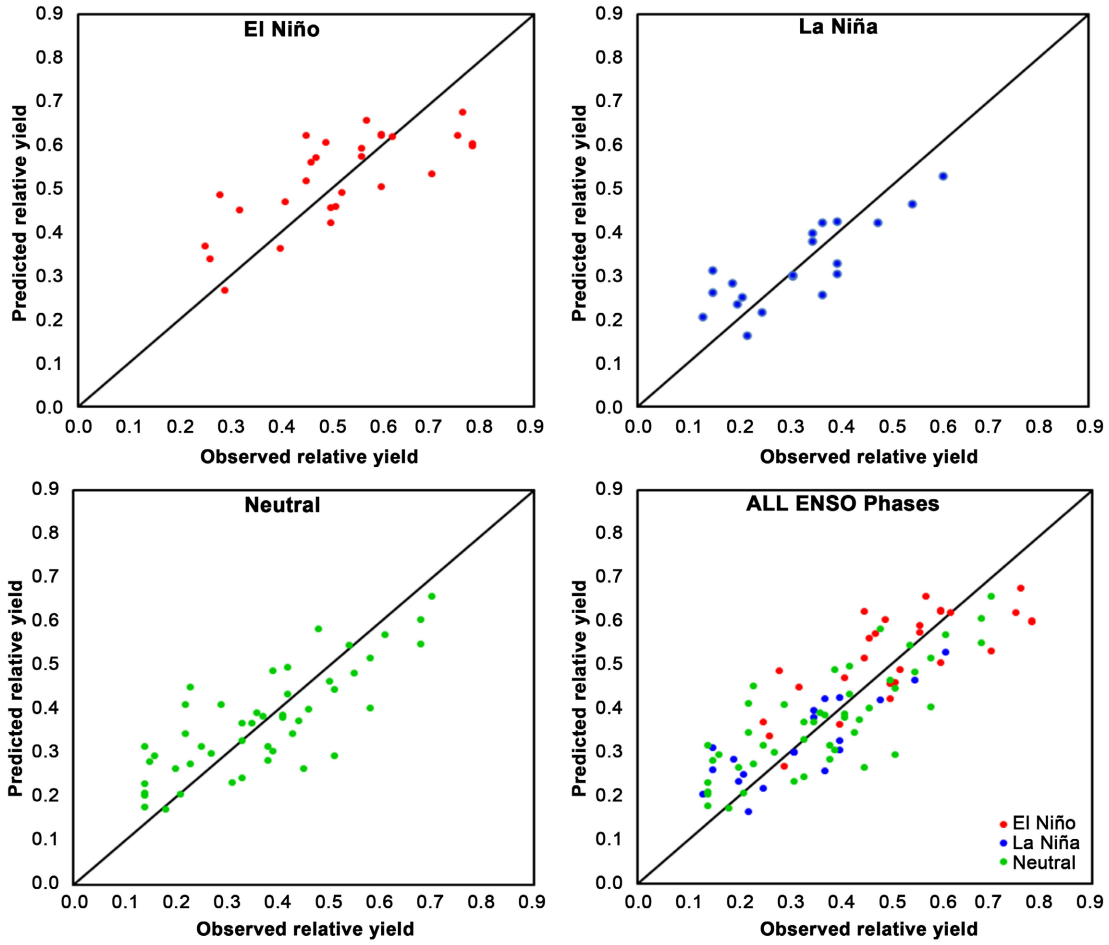

Figure 1. The ENSO phase-specific model-predicted vs. observed values of the relative yield of winter wheat in the Llano Estacado region of the United States (1947-2021).

Table 5. The values of the various measures used to evaluate the generic winter wheat yield model in the Llano Estacado region of the United States under three ENSO phases.

	ENSO phase		
Measures	El Niño	La Niña	Neutral
Mean observed relative yield	0.52	0.32	0.37
Mean predicted relative yield	0.47	0.34	0.41
Mean absolute error	0.10	0.07	0.09
Root mean square error	0.12	0.08	0.11
Willmott Index	0.75	0.89	0.83
Nash-Sutcliffe Index	0.42	0.59	0.51
Percentage error	22	26	30

Relative to the generic yield model, the ENSO phase-specific yield models better reflected the impacts of the interannual variability of weather conditions during the winter wheat growing season in the Llano Estacado region. The following phenomena were the likely reasons for this outcome. The precipitation or drought patterns during a given phenological phase of winter wheat were different across the ENSO phases. For instance, the weather conditions during late fall through early spring in El Niño years were wetter and cooler than the normal years, whereas the La Niña winters were drier and warmer than the normal years [23]-[25]. Accordingly, a phenological phase of wheat occurring during this period may have different responses to drought in El Niño and La Niño years. The sensitivity of wheat yields to water stress under a given ENSO phase was also different across the phenological phases. Because of these phenomena, therefore, the phenological phase-specific drought sensitivity coefficient value was custom-made for a particular ENSO phase, which eventually led to better results.

4. Conclusions

This study developed El Niño-Southern Oscillation (ENSO) phase-specific, Agricultural Reference Index for Drought (ARID)-based yield models for predicting the drought-induced yield loss for winter wheat in Llano Estacado, a semi-arid region in the southern United States. The yield models accounted for the sensitivity of this crop during various phenological phases to drought. The reasonable values of the parameters of each ENSO phase-specific model indicated that the yield models were able to accurately express the relationship between ARID and winter wheat yields in this region as impacted by ENSO. The yield models estimated the drought-induced yield losses reasonably well by reflecting the ENSO phase-specific phenomenon of water stress decreasing the wheat yields in this region.

By using the phenological phase × ENSO phase-specific ARID values obtained from the long-term historical weather data in the ENSO phase-specific yield models (Equations (4) to (6)), various stakeholders in the Llano Estacado region, including wheat growers, extension agents, policymakers, or the scientific community, can estimate the yield loss from drought in an expected ENSO phase-year in advance. The ENSO phase-specific yield models might also be useful for scheduling irrigation allocation tailored to a given ENSO year based on the phenological phase to ensure water access to the phases that are more sensitive to drought.

Conflicts of Interest

The authors declare no conflicts of interest regarding the publication of this paper.

References

[1] Familypedia (2024) Llano Estacado. https://familypedia.fandom.com/wiki/Llano_Estacado

[2] Christensen, J.H., Hewitson, B., Busuioc, A., Chen, A., Gao, X., Held, I., Jones, R.,

Kolli, R.K., Kwon, W.T., Laprise, R., Magaña Rueda, V., Mearns, L., Menéndez, C.G., Räisänen, J., Rinke, A., Sarr, A. and Whetton, P. (2007) Regional Climate Projections. In: Solomon, S., Qin, D., Manning, M., Chen, Z., Marquis, M., Averyt, K.B., Tignor, M. and Miller, H.L., Eds., *Climate Change* 2007: *The Physical Science Basis*, Cambridge University Press, 847-940.
https://www.ipcc.ch/site/assets/uploads/2018/02/ar4-wg1-chapter11-1.pdf

[3] Burke, E.J., Brown, S.J. and Christidis, N. (2006) Modeling the Recent Evolution of Global Drought and Projections for the Twenty-First Century with the Hadley Centre Climate Model. *Journal of Hydrometeorology*, **7**, 1113-1125.
https://doi.org/10.1175/jhm544.1

[4] Karl, T.R., Melillo, J.M. and Peterson, T.C. (2009) Global Climate Change Impacts in the United States. Cambridge University Press.
https://downloads.globalchange.gov/usimpacts/pdfs/climate-impacts-report.pdf

[5] NIDIS (National Integrated Drought Information System) (2022) Southeast Drought Early Warning System (DEWS) Strategic Action Plan 2022-2025. NIDIS.
https://www.drought.gov/sites/default/files/2022-08/2022-2025-southeast-dews-strategic-plan.pdf

[6] Meehl, G.A., Stocker, T.F., Collins, W.D., Friedlingstein, P., Gaye, A.T., Gregory, J.M., Kitoh, A., Knutti, R., Murphy, J.M., Noda, A., Raper, S.C.B., Watterson, I.G., Weaver, A.J. and Zhao, Z.C. (2007) Global Climate Projections. In: Solomon, S., Qin, D., Manning, M., Chen, Z., Marquis, M., Averyt, K.B., Tignor, M. and Miller, H.L., Eds., *Climate Change* 2007: *The Physical Science Basis*, Cambridge University Press, Cambridge, UK.
https://www.ipcc.ch/site/assets/uploads/2018/02/ar4-wg1-chapter10-1.pdf

[7] Herring, D. (2020) How Will Global Warming Harm Natural and Agricultural Resources in the United States?
https://www.climate.gov/news-features/climate-qa/how-will-global-warming-harm-natural-and-agricultural-resources-united

[8] Lettenmaier, D., Major, D., Poff, L. and Running, S. (2008) Water Resources. In: Backlund, P., Janetos, A., Schimel, D., Hatfield, J., Boote, K., Fay, P., Hahn, L., Izaurralde, C., Kimball, B.A., Mader, T., Morgan, J., Ort, D., Polley, W., Thomson, A., Wolfe, D., Ryan, M.G., Archer, S.R., Birdsey, R., Dahm, C., Heath, L., Hicke, J., Hollinger, D., Huxman, T., Okin, G., Oren, R., Randerson, J., Schlesinger, W., Lettenmaier, D., Major, D., Poff, L., Running, S., Hansen, L., Inouye, D., Kelly, B.P., Meyerson, L., Peterson, B. and Shaw, R., Eds., *The Effects of Climate Change on Agriculture*, *Land Resources*, *Water Resources*, *and Biodiversity in the United States*, USDA, 121-150.
https://www.fs.usda.gov/rm/pubs_other/rmrs_2008_backlund_p003.pdf

[9] NIDIS (National Integrated Drought Information System) (2021) Southern Plains Drought Early Warning System (DEWS) Strategic Action Plan 2021-2025. NIDIS.
https://www.drought.gov/sites/default/files/2021-09/2021%E2%80%932025_SP_StrategicPlan.pdf

[10] Woli, P. (2010) Quantifying Water Deficit and Its Effect on Crop Yields Using a Simple, Generic Drought Index. Ph.D. Thesis, University of Florida.
https://ufdc.ufl.edu/ufe0042329/00001

[11] Woli, P., Jones, J., Ingram, K. and Paz, J. (2013) Forecasting Drought Using the Agricultural Reference Index for Drought (ARID): A Case Study. *Weather and Forecasting*, **28**, 427-443. https://doi.org/10.1175/waf-d-12-00036.1

[12] Pandya, P. and Gontia, N.K. (2023) Early Crop Yield Prediction for Agricultural

Drought Monitoring Using Drought Indices, Remote Sensing, and Machine Learning Techniques. *Journal of Water and Climate Change*, **14**, 4729-4746. https://doi.org/10.2166/wcc.2023.386

[13] Woli, P., Jones, J.W., Ingram, K.T. and Fraisse, C.W. (2012) Agricultural Reference Index for Drought (Arid). *Agronomy Journal*, **104**, 287-300. https://doi.org/10.2134/agronj2011.0286

[14] Woli, P., Jones, J.W. and Ingram, K.T. (2013) Assessing the Agricultural Reference Index for Drought (ARID) Using Uncertainty and Sensitivity Analyses. *Agronomy Journal*, **105**, 150-160. https://doi.org/10.2134/agronj2012.0033

[15] Woli, P., Jones, J.W., Ingram, K.T. and Hoogenboom, G. (2014) Predicting Crop Yields with the Agricultural Reference Index for Drought. *Journal of Agronomy and Crop Science*, **200**, 163-171. https://doi.org/10.1111/jac.12055

[16] Philander, S.G. (1990) El Niño, La Niña, and the Southern Oscillation. Academic Press. https://www.sciencedirect.com/bookseries/international-geophysics/vol/46/suppl/C

[17] Hansen, J.W., Jones, J.W., Kiker, C.F. and Hodges, A.W. (1999) El Niño-Southern Oscillation impacts on Winter Vegetable Production in Florida. *Journal of Climate*, 12, 92-102. https://doi.org/10.1175/1520-0442(1999)012<0092:ENOSOI>2.0.CO;2

[18] Hansen, J.W., Hodges, A.W. and Jones, J.W. (1998) ENSO Influences on Agriculture in the Southeastern United States. *Journal of Climate*, **11**, 404-411. https://doi.org/10.1175/1520-0442(1998)011<0404:eioait>2.0.co;2

[19] Steinemann, A.C. (2006) Using Climate Forecasts for Drought Management. *Journal of Applied Meteorology and Climatology*, **45**, 1353-1361. https://doi.org/10.1175/jam2401.1

[20] Baumhardt, R.L., Mauget, S.A., Schwartz, R.C. and Jones, O.R. (2016) El Niño Southern Oscillation Effects on Dryland Crop Production in the Texas High Plains. *Agronomy Journal*, **108**, 736-744. https://doi.org/10.2134/agronj2015.0403

[21] Woli, P., Smith, G.R., Long, C.R. and Rouquette Jr, F.M. (2023) The Niño-Southern Oscillation (ENSO) Effects on Cowpea and Winter Wheat Yields in the Semi-Arid Region of the Southern Us. *Agricultural Sciences*, **14**, 154-175. https://doi.org/10.4236/as.2023.142011

[22] Woli, P., Xue, Q., Smith, G.R., Long, C.R. and Rouquette, F.M. (2024) Estimating the Drought-Induced Yield Loss for Winter Wheat in a Semi-Arid Region of the Southern United States Using a Drought Index. *Agricultural Sciences*, **15**, 812-829. https://doi.org/10.4236/as.2024.158045

[23] Ropelewski, C.F. and Halpert, M.S. (1986) North American Precipitation and Temperature Patterns Associated with the El Niño/southern Oscillation (ENSO). *Monthly Weather Review*, **114**, 2352-2362. https://doi.org/10.1175/1520-0493(1986)114<2352:napatp>2.0.co;2

[24] Kiladis, G.N. and Diaz, H.F. (1989) Global Climatic Anomalies Associated with Extremes in the Southern Oscillation. *Journal of Climate*, **2**, 1069-1090. https://doi.org/10.1175/1520-0442(1989)002<1069:gcaawe>2.0.co;2

[25] Sittel, M.C. (1994) Marginal Probabilities of the Extremes of ENSO Events for Temperature and Precipitation in the Southeastern United States. Technical Report 94-1. Center for Ocean-Atmospheric Studies, the Florida State University, Talla-hassee, Florida. https://apps.dtic.mil/sti/pdfs/ADA284716.pdf

[26] Sittel, M.C. (1994) Differences in the Means of ENSO Extremes for Maximum Temperature and Precipitation in the United States. Technical Report 94-2. Center for

Ocean-Atmospheric Studies, the Florida State University, Tallahassee, Florida.

[27] Acevedo, E., Silva, P. and Silva, H. (2002) Wheat Growth and Physiology. In: Cur-tis, B.C., Rajaram, S. and Gómez Macpherson, H., Eds., *Bread Wheat Improvement and Production*, Food and Agriculture Organization of the United Nations, 39-70.

[28] Undersander, D.J. and Christiansen, S. (1986) Interactions of Water Variables and Growing Degree Days on Heading Phase of Winter Wheat. *Agricultural and Forest Meteorology*, **38**, 169-180. https://doi.org/10.1016/0168-1923(86)90056-0

[29] Howell, T.A., Steiner, J.L., Schneider, A.D. and Evett, S.R. (1995) Evapotranspiration of Irrigated Winter Wheat-Southern High Plains. *Transactions of the ASAE*, **38**, 745-759. https://doi.org/10.13031/2013.27888

[30] McMaster, G.S. and Wilhelm, W.W. (2003) Phenological Responses of Wheat and Barley to Water and Temperature: Improving Simulation Models. *The Journal of Agricultural Science*, **141**, 129-147. https://doi.org/10.1017/s0021859603003460

[31] McMaster, G.S., Wilhelm, W.W. and Frank, A.B. (2005) Developmental Sequences for Simulating Crop Phenology for Water-Limiting Conditions. *Australian Journal of Agricultural Research*, **56**, 1277-1288. https://doi.org/10.1071/ar05068

[32] McMaster, G.S., Green, T.R., Erskine, R.H., Edmunds, D.A. and Ascough, J.C. (2012) Spatial Interrelationships between Wheat Phenology, Thermal Time, and Terrain Attributes. *Agronomy Journal*, **104**, 1110-1121. https://doi.org/10.2134/agronj2011.0323

[33] JMA (1991) Climate Charts of Sea Surface Temperatures of the Western North Pacific and the Global Ocean. Japan Meteorological Agency (JMA).

[34] JMA (2002) Historical El Niño and La Niña Events. Japan Meteorological Agency (JMA), Tokyo, Japan. https://ds.data.jma.go.jp/tcc/tcc/products/elnino/ensoevents.html

[35] Bove, M.C., O'Brien, J.J., Eisner, J.B., Landsea, C.W. and Niu, X. (1998) Effect of El Niño on U.S. Landfalling Hurricanes, Revisited. *Bulletin of the American Meteorological Society*, **79**, 2477-2482. https://doi.org/10.1175/1520-0477(1998)079<2477:eoenoo>2.0.co;2

[36] COAPS (2020) ENSO Index According to JMA SSTA (1868-2020). The Florida State University Center for Ocean-Atmospheric Prediction Studies (COAPS). https://www.coaps.fsu.edu/jma

[37] Nash, J.E. and Sutcliffe, J.V. (1970) River Flow Forecasting through Conceptual Models Part I—A Discussion of Principles. *Journal of Hydrology*, **10**, 282-290. https://doi.org/10.1016/0022-1694(70)90255-6

[38] Willmott, C.J. (1981) On the Validation of Models. *Physical Geography*, **2**, 184-194. https://doi.org/10.1080/02723646.1981.10642213

[39] Day, A.D. and Intalap, S. (1970) Some Effects of Soil Moisture Stress on the Growth of Wheat (*Triticum aestivum* L. Em Thell.). *Agronomy Journal*, **62**, 27-29. https://doi.org/10.2134/agronj1970.00021962006200010009x

[40] Sallam, A., Alqudah, A.M., Dawood, M.F.A., Baenziger, P.S. and Börner, A. (2019) Drought Stress Tolerance in Wheat and Barley: Advances in Physiology, Breeding and Genetics Research. *International Journal of Molecular Sciences*, **20**, Article 3137. https://doi.org/10.3390/ijms20133137

[41] Monteleone, B., Borzí, I., Arosio, M., Cesarini, L., Bonaccorso, B. and Martina, M. (2023) Modelling the Response of Wheat Yield to Stage-Specific Water Stress in the Po Plain. *Agricultural Water Management*, **287**, Article ID: 108444. https://doi.org/10.1016/j.agwat.2023.108444

[42] Li, Z., Zhang, Z. and Zhang, L. (2021) Improving Regional Wheat Drought Risk Assessment for Insurance Application by Integrating Scenario-Driven Crop Model, Machine Learning, and Satellite Data. *Agricultural Systems*, **191**, Article ID: 103141. https://doi.org/10.1016/j.agsy.2021.103141

[43] Lollato, R. (2018) Wheat Growth and Development. MF3300. Kansas State University Agricultural Experiment Station and Cooperative Extension Service. https://bookstore.ksre.ksu.edu/pubs/MF3300.pdf

[44] Musick, J.T. and Dusek, D.A. (1980) Planting Date and Water Deficit Effects on Development and Yield of Irrigated Winter Wheat. *Agronomy Journal*, **72**, 45-52. https://doi.org/10.2134/agronj1980.00021962007200010010x

[45] Acevedo, E. (1991) Morphophysiological Traits of Adaptation of Cereals to Mediterranean Environments. *Improvement and Management of Winter Cereals under Temperature*, *Drought and Salinity Stress*, *Proceedings ICARDA-INIA*, Cordoba, 26-29 October 1987, 85-96.

[46] Acevedo, E., Hsiao, T.C. and Henderson, D.W. (1971) Immediate and Subsequent Growth Responses of Maize Leaves to Changes in Water Status. *Plant Physiology*, **48**, 631-636. https://doi.org/10.1104/pp.48.5.631

[47] Rickman, R.W., Klepper, B.L. and Peterson, C.M. (1983) Time Distributions for Describing Appearance of Specific Culms of Winter Wheat. *Agronomy Journal*, **75**, 551-556. https://doi.org/10.2134/agronj1983.00021962007500030031x

[48] Eastham, J., Oosterhuis, D.M. and Walker, S. (1984) Leaf Water and Turgor Potential Threshold Values for Leaf Growth of Wheat. *Agronomy Journal*, **76**, 841-847. https://doi.org/10.2134/agronj1984.00021962007600050029x

[49] Peterson, C.M., Klepper, B., Pumphrey, F.V. and Rickman, R.W. (1984) Restricted Rooting Decreases Tillering and Growth of Winter Wheat. *Agronomy Journal*, **76**, 861-863. https://doi.org/10.2134/agronj1984.00021962007600050034x

[50] Geng, G., Yang, R., Chen, Q., Deng, T., Yue, M., Zhang, B., *et al.* (2023) Tracking the Influence of Drought Events on Winter Wheat Using Long-Term Gross Primary Production and Yield in the Wei River Basin, China. *Agricultural Water Management*, **275**, Article ID: 108019. https://doi.org/10.1016/j.agwat.2022.108019

[51] Oosterhuis, D.M. and Cartwright, P.M. (1983) Spike Differentiation and Floret Survival in Semidwarf Spring Wheat as Affected by Water Stress and Photoperiod. *Crop Science*, **23**, 711-717. https://doi.org/10.2135/cropsci1983.0011183x002300040026x

[52] Hochman, Z. (1982) Effect of Water Stress with Phasic Development on Yield of Wheat Grown in a Semi-Arid Environment. *Field Crops Research*, **5**, 55-67. https://doi.org/10.1016/0378-4290(82)90006-5

[53] Farooq, M., Hussain, M. and Siddique, K.H.M. (2014) Drought Stress in Wheat during Flowering and Grain-Filling Periods. *Critical Reviews in Plant Sciences*, **33**, 331-349. https://doi.org/10.1080/07352689.2014.875291

[54] Bouaziz, A. and Hicks, D.R. (1990) Consumption of Wheat Seed Reserves during Germination and Early Growth as Affected by Soil Water Potential. *Plant and Soil*, **128**, 161-165. https://doi.org/10.1007/bf00011105

[55] Nicolas, M.E. and Turner, N.C. (1993) Use of Chemical Desiccants and Senescing Agents to Select Wheat Lines Maintaining Stable Grain Size during Post-Anthesis Drought. *Field Crops Research*, **31**, 155-171. https://doi.org/10.1016/0378-4290(93)90058-u

[56] Simane, B., Peacock, J.M. and Struik, P.C. (1993) Differences in Developmental Plasticity and Growth Rate among Drought-Resistant and Susceptible Cultivars of Durum

Wheat (*Triticum turgidum* L. Var. Durum). *Plant and Soil*, **157**, 155-166. https://doi.org/10.1007/bf00011044

[57] Kobata, T., Palta, J.A. and Turner, N.C. (1992) Rate of Development of Postanthesis Water Deficits and Grain Filling of Spring Wheat. *Crop Science*, **32**, 1238-1242. https://doi.org/10.2135/cropsci1992.0011183x003200050035x